High-frequency Instabilities in Hall-effect Thrusters: Correlation with the Discharge Current and Thruster Scale Impact

IEPC-2005-142

Presented at the 29th International Electric Propulsion Conference, Princeton University, October 31 – November 4, 2005

A. Lazurenko*,
Aerothermique Laboratory, CNRS, Orleans, France

L. Albarède**, A. Bouchoule***
GREMI Laboratory, Orleans University, France

High-frequency instabilities (1-10 MHz) were studied experimentally with the use of coaxial probes in Hall-effect thrusters of two types: PPS®-X000ML and double stage Hall thruster. The very general occurrence of such instabilities was confirmed and their main features are in agreement with previous data on other thrusters. Axial localization of these instabilities was found to be dependent on operation mode, with their level independent on discharge current oscillation level. Properties of HF instabilities acquired with a biased probe favor for the hypothesis of electron density fluctuation as origin of these instabilities. The correlation was found between changes of discharge current form and development of these instabilities, and correlation to the electron transport was proposed.

I. Introduction

High-frequency (HF) instabilities from 1-10 MHz range are basic physical phenomena observed in different Hall thrusters.[1-4] Their existence is related to the specifics of Hall thrusters operation – particle flow in the crossed electric and magnetic fields. Some theoretical investigations were undertaken in order to explain the mechanisms of their excitation.[1, 5-7] These HF instabilities are extensively studied in connection with the anomalous transport in Hall thrusters which is not well understood. Recent fully-kinetic PIC modeling of the Hall thruster discharge demonstrated that the electron transport across the magnetic field could be provided by azimuthal electric field fluctuating at these frequencies.[7]

In this article we present recent results of HF instabilities investigation in Hall thrusters of different scale and design: the PPS®-X000 and double-stage Hall thruster. The basic instrument for these investigations is a coaxial Langmuir probe. In comparison with the earlier presented results[4] the spatial properties of instabilities were revealed, as well as their correlation with discharge current oscillation level and its time variation.

II. HF Instabilities in PPS®-X000ML

The PPS®-X000ML thruster is a laboratory model of the SNECMA's high power PPS®-X000 technological demonstrator[8] with a nominal power of 5 kW (Fig. 1) and with the external diameter of the accelerating channel 150 mm. It inherits the design concepts implemented in the PPS®-1350 (Ref 9). In the series of experiments presented here the PPS®-X000ML was equipped with a cathode made by "Fakel".

Instabilities in the PPS®-X000 were studied with the use of coaxial Langmuir probes with a characteristic impedance of 50 Ω. The probe installation on the thruster is shown in Fig. 1. Two probes P1 and P2 are separated axially by 10 mm and installed on the moving arm enabling their displacement in axial direction. The

* Post-doc., lazurenk@cnrs-orleans.fr
** Post-doc., albarede@cnrs-orleans.fr
*** Prof., andre.bouchoule@univ-orleans.fr

probes P1, P3 and P4 are in the same azimuthal plane at initial position $L = L1 \approx 7$ mm from the thruster exit plane and they are separated by ~90° from each other. The probes P1, P2 and P3 are aligned radially with the probe tip's radial position at 5 mm from the channel external radius, whereas the P4 is installed in azimuthal direction. The signals were acquired in the single-shot mode of the digital oscilloscope Tektronix TDS5104.

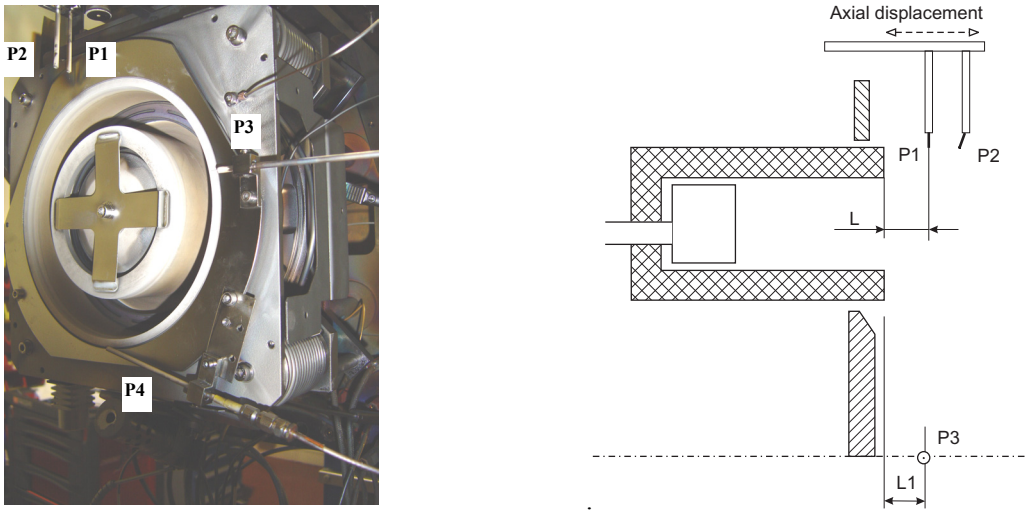

a) View of the PPS®-X000ML with installed coaxial probes;

b) Scheme of the probe installation

Fig. 1. Probe Installation on the PPS®-X000ML.

The typical signal obtained by probes is presented in Fig. 2a as well as the form of the discharge current. The basic features of the signals are close to the properties of HF signal acquired by the antennas in the SPT-100ML[4]. The probes detect the traveling in the azimuthal direction perturbations as can be seen from Fig. 2b where a zoom of the P1 signal from Fig. 2a and the simultaneously acquired P3 signal is presented. The signals have similar forms from where the time delay Δt of the signal P3 relatively the signal P1 can be inferred. Further examining the form and assuming the time delay Δt being one-forth of the time necessary for the perturbation to make one tour around the channel (from the considerations of probe position on the thruster, see Fig. 1) one can approximately indicate the period T_0 of the signal. The strong correlation of the signals is evident from regarding their cross-correlation coefficient function in Fig. 3, where in Fig. 3a its values are represented by gray levels as function of the acquisition time (horizontal axe) and time delay Δt (left axis). The evolution of the time-delay Δt between the signals during the acquisition can be traced by maxima of the cross-correlation coefficient function (dark zones in Fig. 3a). Several curves of the cross-correlation coefficient function at fixed acquisition moments are presented in Fig. 3b. These data were obtained for the operation mode $\dot{m}_a = 5$ mg/s, $U_d = 500$ V.

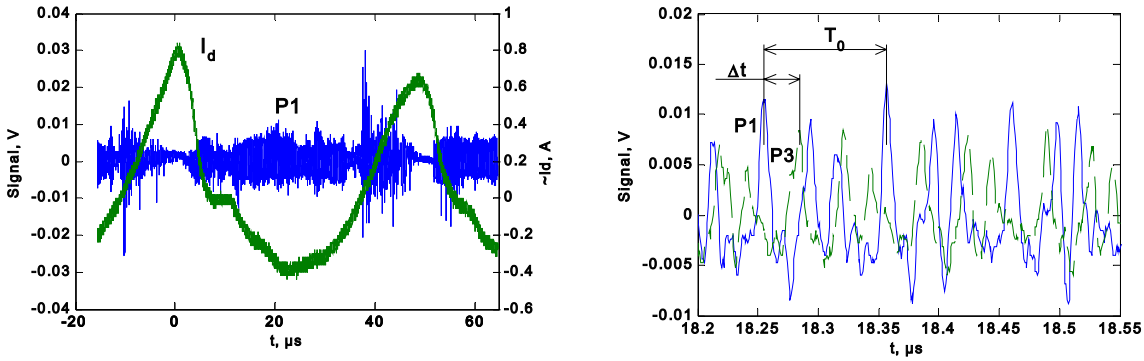

a) Discharge current Id and probe P1 signal;

b) zoom of the P1 and P3 signals;

Fig. 2. Example of the probe signal and discharge current for the PPS®-X000ML.

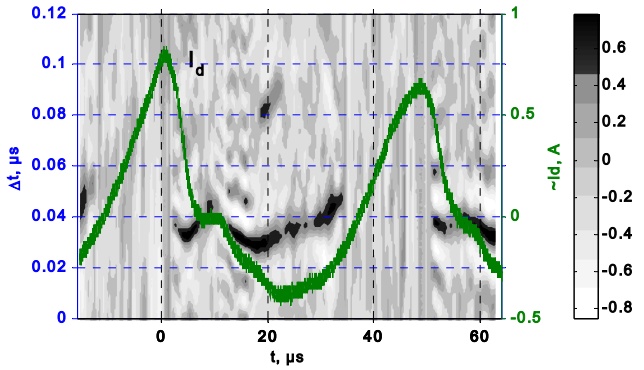

a) cross-correlation function (gray levels) as function of acquisition time (horizontal axis) and time delay between signals (left axis) with the form of discharge current indicated (right axis);

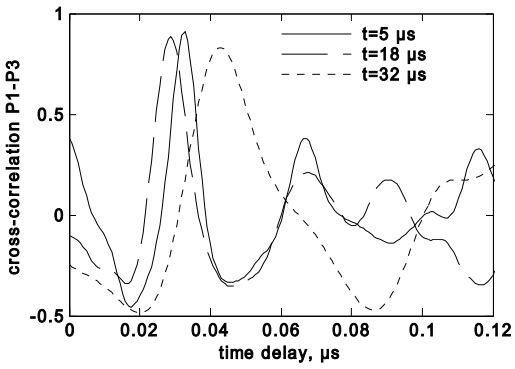

b) cross-correlation curves at some acquisition points;

Fig. 3. Cross-correlation function of the P1-and P3 signals from Fig. 2.

The time delay Δt varies from 0.03 μs to 0.05 μs reaching the minimum at the decreasing front of the discharge current near the its minimum. These Δt values correspond to the azimuthal propagation velocity varying from 4.7×10^6 m/s to 2.8×10^6 m/s.

Axial properties of the instabilities were studied for three discharge voltages U_d = 500 V, 700 V and 900 V at the same mass-flow rate $\dot{m}_a$ = 5 mg/s. Each operation point was optimized by magnetic field to reach the minimum of discharge current. For these discharge parameters the first observation is that the instability level increases with discharge voltage (Fig. 4a). Here the instability level is defined as standard deviation of the total recording. This effect was observed earlier[4] but for the conditions of constant magnetic field. The discharge current also increases with discharge voltage, in spite of magnetic optimization (Fig. 4b, three upper curves). At the same time discharge current oscillation level (defined by corresponding peak-to-peak values) does not follow this tendency, being higher for U_d = 500 V (see Fig. 4b). It seems that instability level correlates with the discharge current value, and not with its oscillation level. The latter will be confirmed by the experimental results on another thruster in this paper. Further observation concerns the position of instability with the maximum level. For the operation mode of U_d = 900 V the maximum instability level is recorded far outside the channel, whereas for U_d = 500 V it seems to be located at not far than 3 mm outside the channel at least (see Fig. 4a).

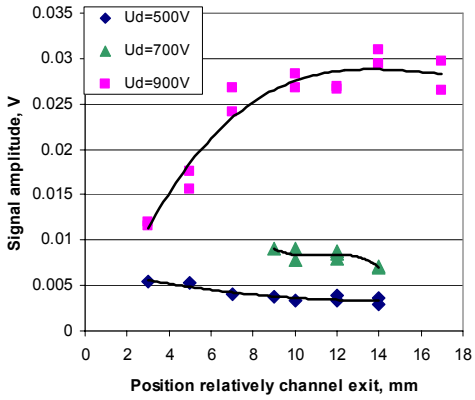

a) Level of P1 probe signal as function of axial position, 3rd degree polynomial fit;

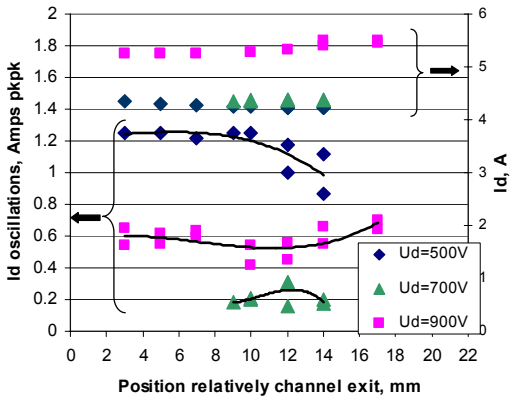

b) Discharge current (three upper curves) and its peak-to-peak values (three lower curves) as function of axial position, 3rd degree polynomial fit;

Fig. 4. Probe signal level and discharge current for the PPS®-X000ML.

The probe signals demonstrated the spatial localization and propagation of the physical source. The fluctuation time-scale (on the order of tens-hundreds nanoseconds) excludes a contribution of ions in such signals. But deriving precise information on plasma fluctuation inducing these signals is not straightforward.

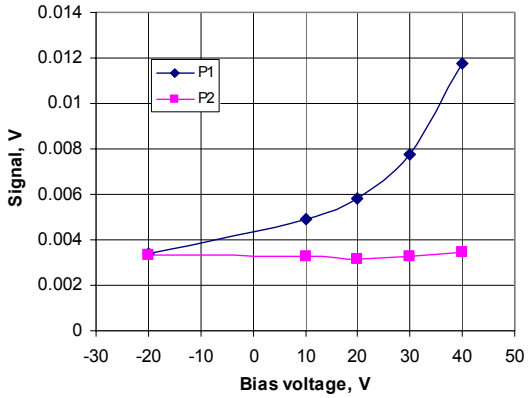

a) Level of P1 and P2 probe signal as function of biasing potential;

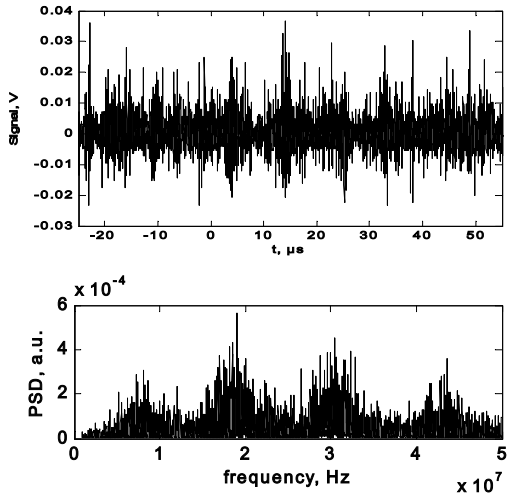

b) Signal P1, U_{bias} = -20 V;

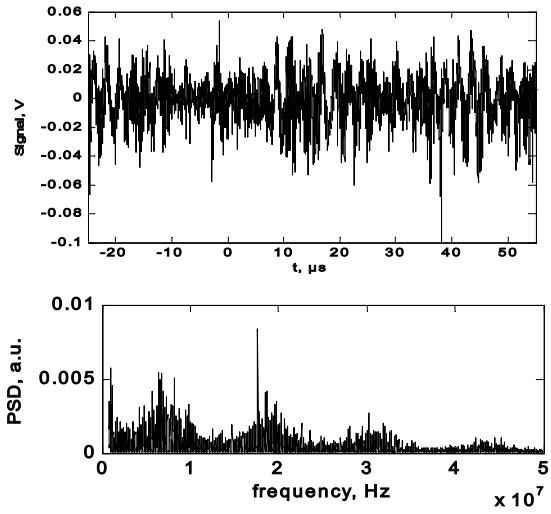

c) Signal P1, U_{bias} = +40 V;

Fig. 5. Biased probe experiment on the PPS®-X000ML.

Two components can be involved in these signals: the first one can be assigned to fluctuations of the electron current on the probe tip and the second one can be induced by potential fluctuations *dV(t)* through the capacitive coupling between the probe and surrounding plasma. To better understand the source of the signals, a study of HF signals was carried out by using DC biased probes. In these experiments, a second probe was used as a reference probe. This probe, labeled P2, was not polarized, remaining at the floating potential. It is located nearby the polarized probe P1 at axial or azimuthal distance of 1 cm.

The biasing potential was applied through the low-frequency branch of the filter box which separates low-frequency and high-frequency components of the signal. These two branches of the box represent classical high-pass (ω = 1 MHz) and low-pass filters, respectively. The signals were acquired in the single-shot mode of the digital oscilloscope Tektronix TDS5104.

In the first experiments, performed on the PPS®-X000ML thruster, the probe P2 was on the same azimuth but displaced axially (see Fig.1). Figure 5a shows the variation of the amplitudes of HF signals derived as a standard deviation of recorded signals. A clear effect is induced by probe biasing: the amplitude of the HF signal of the polarized probe P1 increases while the signal of the reference probe remains almost constant. The P2 constant amplitude gives an indirect indication that the perturbation from the P1 probe is localized in the vicinity of this probe. Fourier analysis shows that the HF content of the signals is not greatly altered (Fig. 5b-c), nevertheless with a relative decrease of higher frequencies contribution.

In the next experimental series the probes were installed on the version of the PPS®-X000 thruster equipped with the discharge chamber which had followed ~200 hours of tests. The reference P2 probe was installed azimuthally at 1 cm from the biased P1 probe. The amplitude of biased probe signal follows the same evolution as in the first experiments. It can be speculated that biasing the probe negatively blocks the component due to the electron current fluctuations and therefore the probe signal in this case is mostly due to the fluctuations of plasma potential. In contrast, high positive biasing potential favors for electron current collection, therefore at these conditions this component could be the most important. The form of the signals at different biasing voltages was compared (Fig. 6). At -20V biasing potential the forms of signals are very close. The floating potential at the zone of probe location is -15…-20 V relatively to the

ground. Therefore, biasing probe to -20 V is equivalent to the working conditions of the unbiased probe. A more complicated picture is observed at biasing potential +40 V, with the unbiased probe signal having higher frequency components (Fig. 6b). It is clear that biasing effects change significantly the shape of probe signals. In terms of signal shape, or Fourier spectrum, the two contributions have different features. Plasma potential fluctuations, in this frequency range, are linked to electron density fluctuations. If we assume a linear relationship between *dNe(t)* and *dV(t)*, then the capacitive contribution to the probe signal should contain higher frequencies, induced by the *d/dt* character of this contribution. This effect seems to be observed in the two experiments (frequency spectrum in Fig. 5c and in Fig. 6). But further investigations remain clearly necessary to confirm such conclusions.

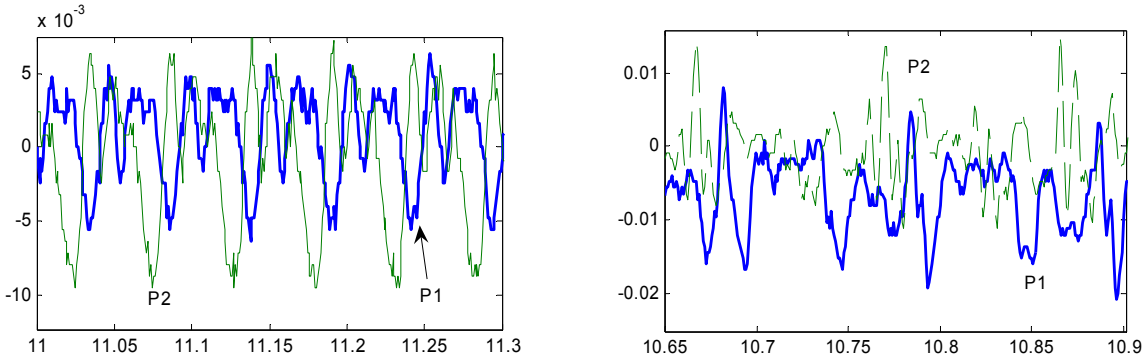

a) biasing potential -20 V; a) biasing potential +40 V;

Fig. 6. Form of the signals from the biased and unbiased probes on PPS®-X000.

Another effect was observed at these biased probe experiments: a 100-400 kHz modulation of the HF signal appears (see Fig.5b-c) at high positive potentials (> +20V). Taking into account the filter characteristics this modulation is even stronger than recorded. Oscillations from this frequency band are often referenced as "transit-time" oscillations (see Ref. 10). Analysis of this effect is also underway.

III. HF Instabilities in double-stage Hall thruster

Double-stage Hall effect thruster (DSHET), studied here, is a 1.5 kW one with separated ionization and acceleration zones.[11] Instabilities in the DSHET were studied with the use of coaxial Langmuir probes with a characteristic impedance of 50 Ω, as for the previous thruster. The probe installation on the thruster is shown in Fig. 7. Probes P1 and P2 are aligned axially at the distance of 11 mm; probes P1, P3 and P4 are in the same azimuthal plane at 4 mm from the thruster exit plane.

The probe signals in the double-stage thruster are strongly modulated with a high frequency from the range of 50-150 MHz (Fig. 8 and Fig. 9), but the lower frequencies from the range of 1-15 MHz are clearly visible. It is on this longer time-scale that the signals from azimuthally separated probes are time-delayed (see Fig. 8a) with $\Delta t \sim 0.03$ μs. The inferred azimuthal propagation velocity is 2.6×10^6 m/s (for 50 mm of channel radius). The value of Δt corresponds to those ones observed earlier in the PPS®-X000ML (Part II) and in the SPT-100ML.[4] Thus, also in the case of double-stage thruster there exist azimuthal waves that could be most likely associated with drift waves. It should be nevertheless noted that the correlation between signals from probes separated azimuthally on 90° is not generally high indicating that low-frequency component is not stable.

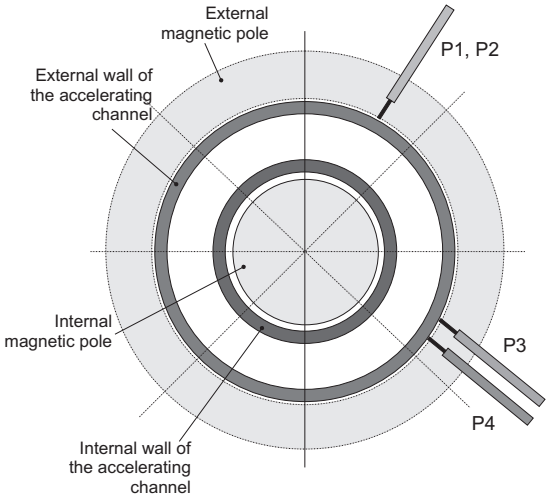

Fig. 7. Positions of probes on the double-stage Hall thruster.

The high frequency content of the probe signal (f>20 MHz) seems to be dependent on the magnetization current I_b in the rear thruster coil (see Fig. 8b and Fig. 9), shifting to the lower-frequency domain with a higher magnetization current.

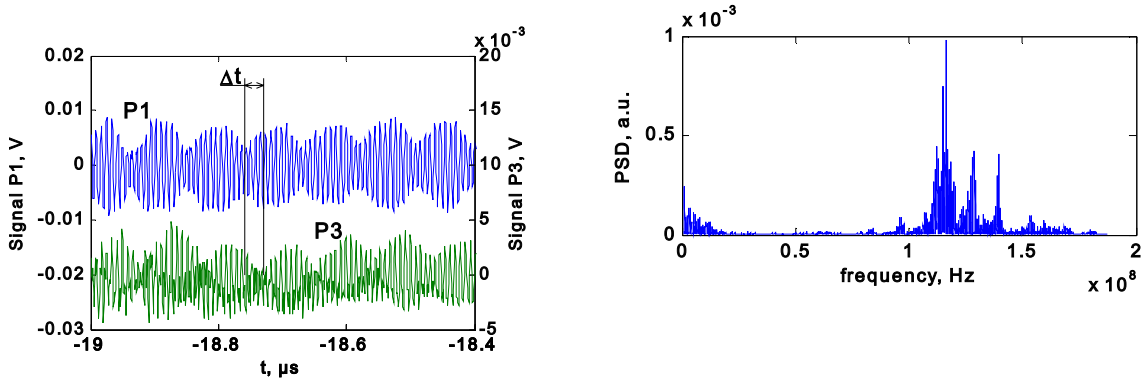

a) signals from probes P1 and P3; b) Fourier transform of P1 signal;

Fig. 8. Signals from the probes in the double-stage Hall thruster at I_b = 1 A.

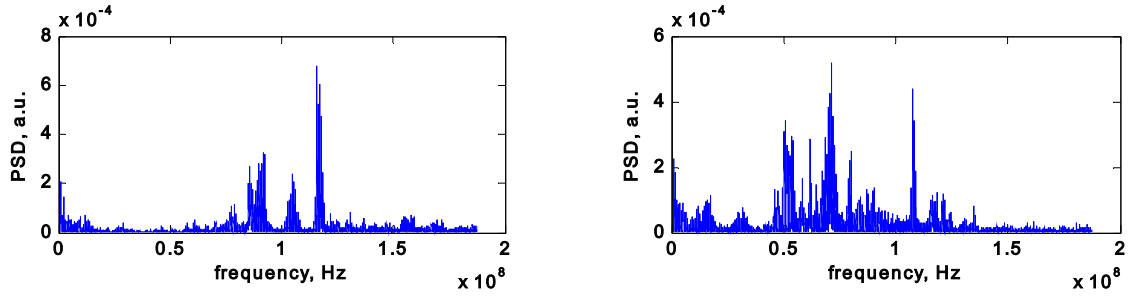

a) I_b = 3 A; b) I_b = 7 A;

Fig. 9. Fourier transforms of P1 signals at different I_b currents in the double-stage Hall thruster.

The correlation between discharge current oscillation level (defined again by peak to peak value) and instability oscillation level (defined as standard deviation of the signal recording) was studied utilizing the following procedure. An alternate component of discharge current was delivered to one of the oscilloscope entrances. The oscilloscope was triggered on a certain level of discharge current oscillations with the simultaneous acquisition of probe signals. The signals were then post-analyzed to calculate the instability level. The instability level does not show any distinct dependence on discharge current oscillation level for the investigated operation modes (Fig. 10, operation mode $\dot{m}_a$ = 4 mg/s, U_d = 350 V), with the maximum deviation of ~30% relatively middle value for all experimental points.

The next step was to investigate a correlation between discharge current I_d, its time derivative $D = \frac{dI_d}{dt}$ and signal amplitude σ. The averaged signal amplitude was calculated with a rectangular moving window of length N with 50 % overlapping:

$$\sigma_k = \left(\frac{1}{N-1} \sum_{i=1}^{N} (s_i - \bar{s}_k)^2 \right)^{1/2}, \quad (1)$$

where s – signal and $\bar{s}_k = \frac{1}{N} \sum_{i=1}^{N} s_i$. The averaging was performed over a period equal to 2-3 times needed for a perturbation to make a tour around the channel with the assumed wave propagation velocity, i.e. ~0.4μs. This procedure allows tracking a variation of the signal amplitude at this time-scale. Then the cross-correlation coefficient function was calculated for $D = \frac{dI_d}{dt}$ and σ.

$$R_{D,\sigma}(k) = \frac{C_{D,\sigma}(k)}{\sqrt{C_{D,D}(k) C_{\sigma,\sigma}(k)}}, \quad (2)$$

where $C_{D,\sigma}(k)$ - cross-covariance function and $C_{D,D}(k)$, $C_{\sigma,\sigma}(k)$ corresponding auto-covariance functions. In agreement with earlier observations[3,4], the instabilities develop significantly when $\frac{dI_d}{dt} < 0$, i.e. at the decreasing front of discharge current (Fig. 11). The cross-correlation coefficient function has a minimum at few μ-seconds

after zero indicating that generally the instabilities develop a few μ-seconds after the discharge current inflection point at the decreasing front where discharge current time derivative has its minimum.

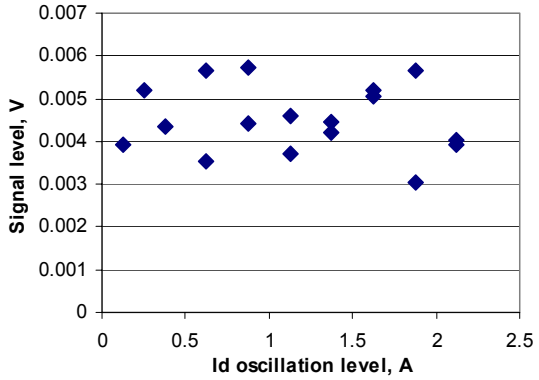

Fig. 10. Instability level as function of discharge current oscillation level in the double-stage Hall thruster.

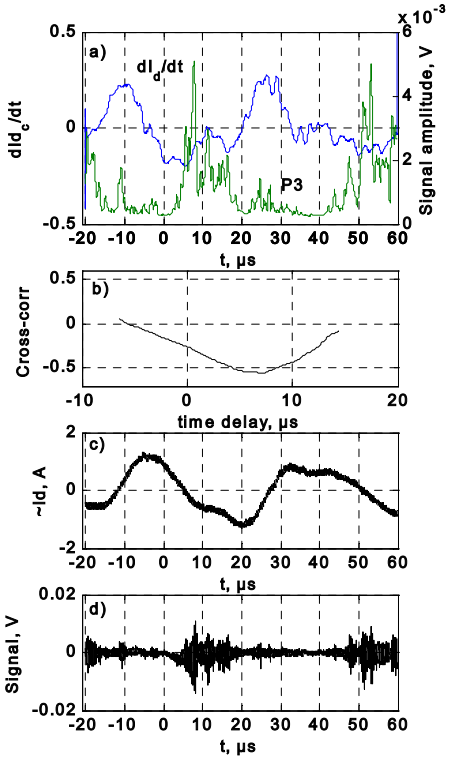

Fig. 11. Instability amplitude and correlation with discharge current derivative in the double-stage Hall thruster.

IV. Discussion

HF instabilities were studied in two different types of Hall thrusters: the PPS®-X000ML and the DSHET . Along with earlier studies (Ref. 1-4) it proves that these HF instabilities have a general character related to the basic physics of Hall thruster discharge.

At the same time the character of these instabilities varies significantly. In SPT-100ML thruster we observed these instabilities in the form of well-localized peaks. From this space-time variation it was relatively simply to define their period and azimuthal mode. In the case of the PPS®-X000ML thruster such a well-defined structure can be found only for some operating points (as for example in Fig. 2). For other operation modes (U_d, I_b, $\dot{m}_a$) of the thruster the higher wave numbers (> 100 m^{-1}) are predominant in the probe signal. The signals from azimuthally separated probes (as P1 and P3 in Fig. 1) can have weak correlation or even have not any correlation. It can indicate that azimuthally propagating waves are unstable. Even more complicated picture is observed in the DSHET where the signals have a very strong high frequency > 50 MHz modulation (see Fig. 8-9). Expected 1-10 MHz instabilities are observed as lower-frequency components of the signals which are time delayed in two azimuthally separated probes. Progressive evolution of the frequency content of probe signal with increasing magnetization current suggest that this higher-frequency component could be also related to the discharge physics.

Biased probes give additional information on the HF signal. The signal amplitude increases with more positive biasing potential whereas the HF content of the signal practically does not change (see Fig. 5). Biasing probe positively favors for collection of electron current from the plasma. Therefore, in our experiments with the biased probe the effects of current collection from the plasma give a greater contribution to the signal than the capacitive effects.

One of the primary reasons of studying these HF instabilities is their relation to the electron dynamics and therefore to the electron transport in Hall thrusters. Experimental data show that in the presence of the HF instabilities the form of discharge current is modified (Fig. 12); it becomes more flat than when there are no instabilities. This change in inclination could indicate an additional transport due to the anomalous electron conductivity.

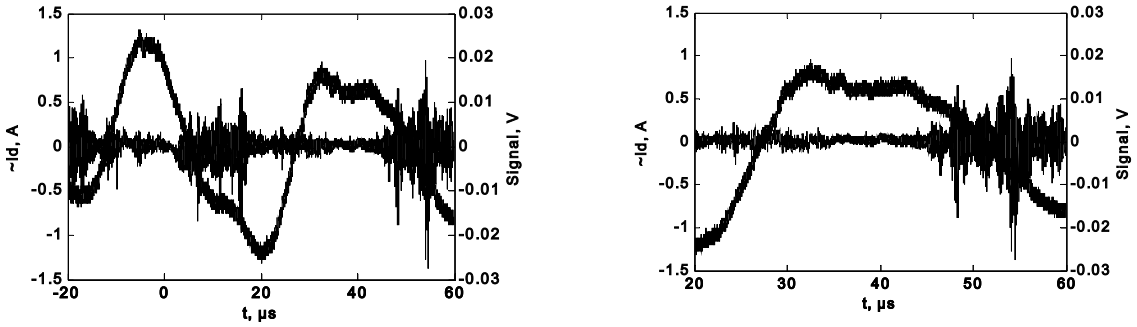

a) total recording; b) zoom;

Fig. 12. Discharge current and probe signal in the double-stage Hall thruster.

Conclusions

New experimental insights into HF instabilities confirm their general character related to the physics of discharge in Hall thruster. They also give additional arguments in favor of hypothesis that in their origin – the perturbations of electron density. Further investigation of these instabilities, in particular their quantitative relation to the electron transport, requires, from our point of view, a deeper theoretical description.

Acknowledgments

The authors acknowledge the technical support of P. Lasgorceix, C. Legentil and S. Sayamath. This work was performed in the frame of the French research group GDR n°2759 CNRS/CNES/SNECMA/Universities "Propulsion Spatiale à Plasma". The participation of A. Lazurenko and L. Albarede was funded by a fellowship from the SNECMA, France.

References

[1] Y.V. Esipchuck and G.N. Tilinin, "Drift instability in a Hall-current plasma accelerator", Sov. Phys. Tech. Phys. **21**(4), 417 (1976).

[2] A.A. Litvak, Y. Raitses, and N.J. Fisch, "Experimental studies of high-frequency azimuthal waves in Hall thrusters", Phys. Plasmas, **11(**4), 1701 (2004).

[3] Prioul, M., "Experimental Study of Hall Thrusters", PhD thesis University of Orléans, September 2002.

[4] A. Lazurenko, V. Vial, M. Prioul, and A. Bouchoule "Experimental investigation of high-frequency drifting perturbations in Hall thrusters", Physics of Plasmas, **12**(1), 013501 (2005).

[5] V. Baranov, Yu. Nazarenko, and V. Petrosov "Azimuthal Non-uniformities in Accelerators with Closed Eelectron Drift", paper IEPC-01-18 at 27 International Electric Propulsion Conference, Pasadena, USA, 15-19 October, 2001.

[6] A.A. Litvak and N.J. Fisch, "Rayleigh instability in Hall thrusters", Phys. Plasmas, **11(**4), 1379 (2004).

[7] J.C. Adam, A. Héron, and G. Laval, "Study of stationary plasma thrusters using two-dimensional fully kinetic simulations", Phys. Plasmas **11**, 295 (2004).

[8] O. Duchemin, P. Dumazert, N. Cornu, D. Estublier, F. Darnon "Stretching the Operational Envelope of the PPS®X000 Plasma Thruster", paper AIAA-04-3605 at the 40th Joint Propulsion Conference, USA, 2004.

[9] M.Prioul, F.Marchandise, P.Dumazert et al "PPS®-1350 qualification status and performances", 4th International Spacecraft Propulsion Conference, Sardinia, Italy, 2004.

[10] E.Y. Choueiri, "Plasma oscillations in Hall thrusters", Phys. Plasmas, **8**(4), 1411 (2001).

[11] C. Boniface, G.J.M. Hagelaar, L. Garrigues, J.P. Boeuf, M. Prioul "Numerical study of a Double Stage Hall Effect Thruster", presented at the IEPC-2005, Princeton, USA, 2005.